SHARE: SoH-Aware Reconfiguration to Enhance Deliverable Capacity of Large-Scale Battery Packs

Liang He[1], Yu Gu[2], Ting Zhu[3], Cong Liu[4], Kang G. Shin[1]
[1]The University of Michigan, Ann Arbor, MI, USA
[2]IBM Research, Austin, TX, USA
[3]The University of Maryland, Baltimore County, ML, USA
[4]The University of Texas at Dallas, TX, USA

ABSTRACT

Unbalanced battery cells are known to significantly degrade the performance and reliability of a large-scale battery system. In this paper, we exploit emerging reconfigurable battery packs to mitigate the cell imbalance via the joint consideration of system reconfigurability and State-of-Health (SoH) of cells. Via empirical measurements and validation, we observe that a significantly larger amount of capacity can be delivered when cells with similar SoH levels are connected in series during discharging, which in turn extends the system operation time. Based on this observation, we propose two SoH-aware reconfiguration algorithms focusing on fully and partially reconfigurable battery packs, and prove their (near) optimality. We evaluate the proposed SoH-aware reconfiguration algorithms using both experiments and simulations. The algorithms are shown to deliver about 10–30% more capacity than SoH-oblivious configuration approaches.

Categories and Subject Descriptors

C.3 [**Process control systems**]: Miscellaneous

General Terms

Design

Keywords

Reconfigurable battery packs, state-of-health, cell imbalance

1. INTRODUCTION

Large-scale battery packs are widely adopted in diverse applications such as electric vehicles and aircraft [2,6], thanks to their ability to support loads with high energy and power requirements. However, with the increasing battery pack scale, they also incur new challenges such as increased management complexity and higher rate of cell failures [9, 24].

To address these challenges, the concept and implementation of reconfigurable battery packs have recently been proposed and investigated [7, 15, 26–28, 37]. With reconfigurable battery packs, the connectivity among individual cells can be actively altered according to the real-time load requirements and system states such as cell voltage levels. Higher energy-efficiency of battery packs can thus be achieved by controlling how and which of the cells should be charged/discharged/rested. Significant research efforts have been devoted in this direction, such as achieving high reconfigurability with low system complexity [22], matching the supplied and desired load voltage levels in real time [17], making a tradeoff between the cycle efficiency and capacity utilization of the battery pack [29], and charging the cells in the battery pack to their full capacity [18].

Besides the above issues, one of the most common operation challenges for large-scale battery packs is the cell imbalance [20, 22]. Due to various uncontrollable factors such as electrolyte decomposition, active material dissolution, passive film formation, manufacturing, and operation environments, the capabilities of individual cells within a pack to accept and provide charge (termed as *State-of-Health* (SoH) of cells) tend to differ from each other over usage and time. The unbalanced cells degrade the pack's performance. In particular, during discharging, the weakest cell (i.e., the cell with the lowest SoH level) in a set of series connected cells (i.e., a cell string) dominates the capacity that the string can deliver. Further discharge of the string beyond this limit may cause the weakest cell to suffer dramatic heating issue, which may eventually risk the safety of the entire system. Although there have been many proposals for the discharge management of reconfigurable battery packs, the cells' SoH, despite its importance, has received far less attention in the literature. To remedy this deficiency, we propose the joint consideration of system reconfigurability and cells' SoHs to mitigate the cell imbalance when discharging.

From both existing literature and our empirical measurements, we observe that by connecting cells with similar SoH levels in series, i.e., making cells with similar SoH share the same string, a significantly more power capacity can be delivered from the battery system, especially with severe cell imbalance. Based on this observation, we propose SHARE-Full and SHARE-Partial, two SoH-Aware REconfiguration algorithms to determine a proper system configuration based on the real-time cell SoH levels, focusing on the fully and partially reconfigurable battery packs. The main contributions of this paper are three-fold.

- To the best of our knowledge, this is the first joint consideration of system reconfigurability and cell SoH levels to maximize the energy delivery of battery packs.
- For battery packs with full reconfigurability, we introduce SHARE-Full, an optimal algorithm for identify-

ICCPS '15, April 14 - 16, 2015, Seattle, WA, USA

http://dx.doi.org/10.1145/2735960.2735967.

ing the system configuration with the maximal deliverable capacity. For battery packs with partial reconfigurability, we prove the NP-hardness of the problem by deducing it from the maximum-weight independent set problem based on a graph-based problem transformation. Furthermore, we propose SHARE-Partial, a greedy solution and prove its near-optimality.

- We perform both experiments and simulations to evaluate the proposed SoH-aware reconfiguration algorithms. The results show about 10%–30% more capacities can be delivered with the SoH-aware configurations. These improvements are significant especially when considering the slow advances of battery technologies, e.g., less than 3× improvement in energy density since 1990 [8].

The paper is organized as follows. The basic concepts and motivation are introduced in Sections 2 and 3, respectively. The SoH-aware configuration algorithms for fully and partially reconfigurable battery packs are presented in Sections 4 and 5, respectively. The evaluation results are reported in Sections 6 and 7. We discuss a practical issue in Section 8. Section 9 reviews the related literature. The paper concludes in Section 10.

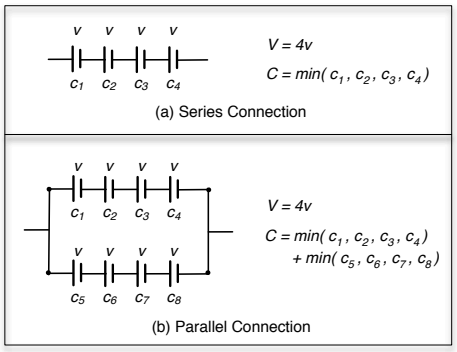

Figure 1: Series and parallel connection of cells.

2. PRELIMINARIES

2.1 Series and Parallel Connection of Cells

In general, cells in a battery pack can be connected in series or in parallel. The series connection of cells (i.e., cell string) increases the supplied voltage but its deliverable capacity is dominated by the weakest cell in the string. On the other hand, connecting cells in parallel does not increase the supplied voltage but achieves higher deliverable capacity. For example, when connecting four cells in series as shown in Fig. 1(a), the supplied voltage is the sum of the four cells, while the deliverable capacity is dominated by the cell of the least capacity. On the other hand, connecting multiple cell strings in parallel achieves a capacity that is equal to the sum of their respective deliverable capacities (Fig. 1(b)).

2.2 Cell Imbalance and State-of-Health

Due to many uncontrollable factors such as manufacturing, surrounding environment, and cycling differences, the strengths of cells in a battery pack will be different over time and usage. This is commonly referred to as the *cell unbalance issue* in a pack. The cell imbalance significantly degrades the performance of the pack, especially for cells connected in series where the string strength is dominated by the weakest cell, as mentioned in Section 2.1.

To clearly observe the cell imbalance problem, we disassembled a 6-cell Lithium-ion battery pack used in the Lenovo Thinkpad X220i laptop and discharged them individually with a current of 2,300 mA until the 2.8 V cut-off voltage is reached. The delivered capacities of the six cells are plotted in Fig. 2. The maximum and minimum delivered capacities are shown to be 1,481.8 mAh and 1,233.8 mAh, respectively, indicating as high a difference as 20.1%.

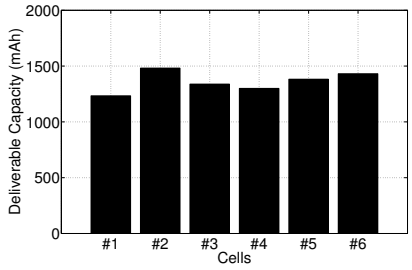

Figure 2: Delivered capacities of cells in a laptop battery.

The State-of-Health (SoH) of cells, normally presented in percentages, is a widely adopted metric to quantify the cell strength during their life cycles. Taking the new cell as of 100% SoH, a fully charged 2,300 mAh cell with 80% SoH can only deliver a capacity of about $2,300 \times 80\% = 1,840$ mAh. The real-time estimation of cell SoH levels has been studied extensively [10, 40] and is supported by many commercial battery management systems [34]. Obviously, the variance of cells' SoH levels is a good indicator of the cell imbalance degree in a pack.

2.3 Reconfigurable Battery Packs

Here we want to address the cell imbalance problem with the reconfigurable battery packs, in which the connectivity among cells (e.g., in series or in parallel) can be actively altered. The alterability of cell connectivity allows us to jointly determine the battery pack configuration based on the cell SoH levels and the load requirements (i.e., SoH-aware (re)configuration) in order to maximize the deliverable capacity of battery packs.

Specifically, a reconfigurable battery pack can be represented by a weighted directed graph $\mathcal{G} = \{\mathcal{V}, \mathcal{E}, \mathcal{W}\}$ [17], where

- each vertex in $\mathcal{V}$ represents a cell in the system, and thus $|\mathcal{V}| = N$ where N is the total number of cells in the battery pack;
- $\mathcal{E}$ reflects how these cells can be connected to each other and thus captures the system reconfiguration flexibility: an edge $v_i \rightarrow v_j \in \mathcal{E}$ if and only if the two corresponding cells can be directly connected according to the current direction in the battery pack;
- the weight set $\mathcal{W}$ on the vertices captures the SoH levels of cells in the battery pack[1].

[1]The weight of vertices can be defined according to the problem tackled. For example, instead of the cell SoH levels as in this work, $\mathcal{W}$ is defined as the real-time cell voltages in [17] to facilitate the matching between the supplied and the load required voltage levels.

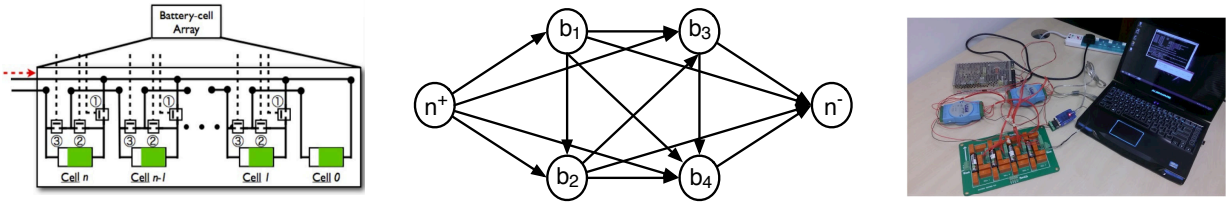

(a) Battery pack design (b) Graph representation (c) Testbed implementation

Figure 3: Graphic representation of a reconfigurable battery pack and the implementation of our 4-cell reconfigurable battery board according to [22].

Figs. 3(a) and 3(b) show an example of the graph representation of a 4-cell reconfigurable battery pack designed according to [22], and Fig. 3(c) shows our corresponding prototype implementation [19]. This graph representation allows us to capture the reconfiguration flexibility offered by the battery pack, facilitating the design of a SoH-aware reconfiguration algorithm using graph theory, as we will show in Section 5.

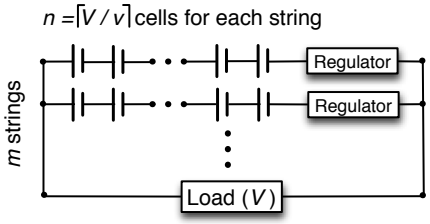

Figure 4: System model.

2.4 System Model and Application Scenario

In this paper, we consider the system model shown in Fig. 4. The battery pack consists of N cells each with nominal capacity c. A voltage output of V is required by the load, indicating a number of $n = \lceil \frac{V}{v} \rceil$ cells are required to form a series string, where v is the nominal voltage of cells. A total of m ($m \leq N/n$) such strings are connected in parallel to supply the load together. Because cell voltage may not always be the nominal voltage v during discharging, to provide a stable voltage output, a voltage regulator is added in each string. This is also the common approach to handle the cell voltage changes in battery pack products [1, 41].

Fig. 5 shows the application scenario considered in this paper. After charging, the battery pack is reconfigured based on the cells' SoH levels, and then the battery pack is used to support the load (i.e., discharging). A real-life example for this scenario is to reconfigure the battery pack after charging an electric vehicle during night time at home, and then drive it to work the next day. It is also possible to reconfigure the battery pack during discharging when necessary. The cell information during the charging and discharging processed are logged, based on which the cells' SoH levels are estimated. Our objective is to design SoH-aware reconfiguration algorithms to identify the proper system configuration based on the real-time SoH levels of cells (as highlighted in Fig. 5), which increases the deliverable capacity of the battery pack and thus extends the system operation time.

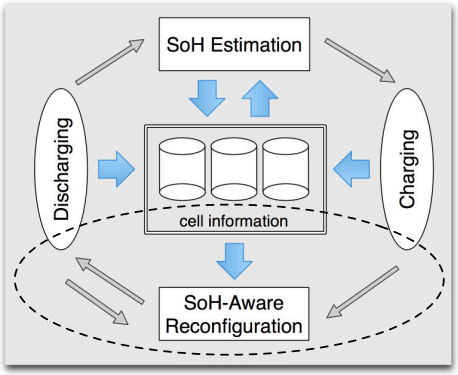

Figure 5: Application scenario.

3. MOTIVATION

To clearly demonstrate how the cell imbalance degrades the battery pack performance, let us consider the example shown in Fig. 6(a) consisting of four cells with nominal capacity of 2,300mAh. Two of the cells (i.e., A and B) are of 100% SoH and can deliver a full capacity of 2,300mAh upon fully charged. On the other hand, cell C and D are of only 80% SoH levels, indicating a deliverable capacity of 1,840mAh with a single charge. When the four cells are connected into the SoH-oblivious configuration $\overline{AC}||\overline{BD}$ as shown in Fig. 6(b)[2], only 1,840mAh capacity can be delivered from each string because the deliverable capacity is determined by the weakest cell (i.e., cell C and D in their respective string). Therefore, the SoH-oblivious configuration can only deliver about $1,840 \times 2 = 3,680$mAh capacity, and the remaining capacity of $2,300 - 1,840 = 460$mAh in cell A and B cannot be effectively utilized.

On the other hand, if cells with similar SoH levels are organized to share the same string, i.e., the SoH-aware configuration $\overline{AB}||\overline{CD}$ (as in Fig. 6(c)), an amount of 2,300mAh and 1,840mAh capacity can be delivered by string $\overline{AB}$ and $\overline{CD}$, respectively. This leads to a total delivered capacity of 4,140mAh and about $\frac{4,140-3,680}{3,680} = 12.5\%$ increase when compared with the SoH-oblivious configuration in Fig. 6(b).

Besides the illustrative example shown in Fig. 6, we empirically compare the delivered capacities with the SoH-aware and the SoH-oblivious configurations with four 2,300mAh AA rechargeable cells. Two of them have been in extensive usage since March 2013 (and thus with lower SoH levels) and the other two are brand new for the measurements (and thus with higher SoH levels). We fully charge the cells with the associated commercial chargers, and then these four cells are connected in the SoH-oblivious and SoH-aware configurations as shown in Fig. 6(b) and Fig. 6(c). We adopt the

[2]In this notation, the overline indicates the series connection, and || represents the parallel connection.

Cell	A	B	C	D
SoH (%)	100	100	80	80
Capacity (mAh)	2,300	2,300	1,840	1,840

Nominal capacity: 2,300 mAh

(a) four cells with the same nominal capacity but different SoH

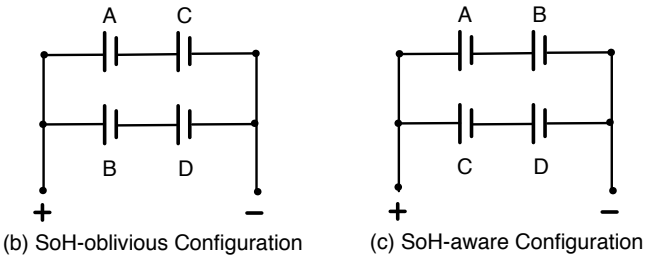

(b) SoH-oblivious Configuration (c) SoH-aware Configuration

Figure 6: Necessity of SoH-aware configuration.

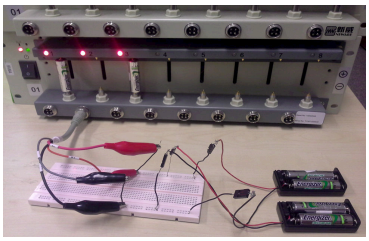

Figure 7: Measurement settings with four AA rechargeable cells.

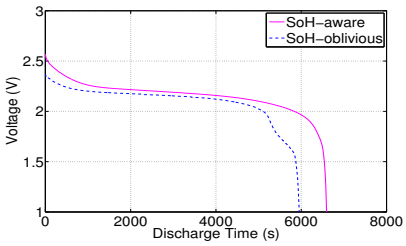

Figure 8: Voltage curves during the discharge processes.

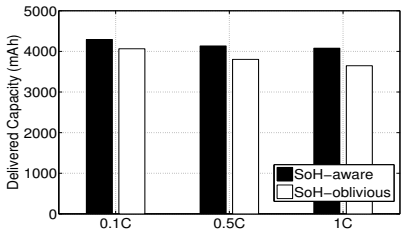

Figure 9: Delivered capacities with different discharge currents.

Table 1: SoH-aware v.s. SoH-oblivious.

Configuration	SoH-aware	SoH-oblivious
Capacity (mAh)	4,078.4	3,647.1

NEWARE battery tester [5] to discharge these cells with a constant current of 1C (i.e., 2,300mA) and monitor the discharge processes. Fig. 7 presents our measurements settings. Table 1 lists the delivered capacities with the two configurations. One can see that the SoH-aware configuration can deliver about 11.8% more capacity when compared with the SoH-oblivious configuration. Fig. 8 plots the voltage curves during the discharge processes. We also repeat the measurements with different discharge currents of 0.1C (i.e., 230mA) and 0.5C (i.e., 1,150mA). The delivered capacities (together with that obtained with 1C discharge current) are shown in Fig. 9. One can see the SoH-aware configuration delivers more capacity than the SoH-oblivious configuration in all three cases, especially with larger discharge currents.

These results demonstrate the fact that in order to increase the deliverable capacity of battery packs and thus extend the system operation time, *only cells with similar SoH levels should be connected in series and thus share the same string*. In the following two sections, we will introduce our design on the SoH-aware reconfiguration focusing on a fully (i.e., the connectivity among cells is fully reconfigurable) and a partially (i.e., only a constraint reconfigurability is offered) reconfigurable battery packs, respectively.

4. BATTERY PACKS WITH FULL RECONFIGURABILITY

In this section, we investigate the SoH-aware reconfiguration when the battery pack is fully reconfigurable, i.e., the cells in the battery pack can be arbitrarily connected. In practice, this is the case when the battery pack can be safely removed from the load, and the cells in the pack can be reconfigured offline.

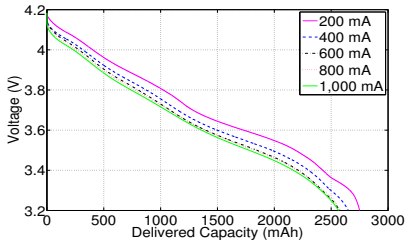

Figure 10: Rate-capacity effect: less capacity is delivered with larger discharge currents.

4.1 Problem Formulation

With the graph representation of battery packs, a fully reconfigurable battery pack can be captured by a fully connected graph, and any subset of cells in the pack can be connected in series. As a result, a total number of $m = \lfloor \frac{N}{n} \rfloor$ disjoint cell strings $\{s_1, s_2, \cdots, s_m\}$ can be formed. In this way, the challenge resides in how to construct such m strings to maximize the capacity delivery.

Note that the requirement on the disjoint cell strings is to avoid including the same cell into multiple strings, in which case the discharge currents of the shared cell would be larger than other non-shared cells. This is not desirable because of two reasons. First, the heterogeneous discharge currents among cells makes the cell imbalance more severe. Second, the much larger discharge current of the shared cell degrades its capacity delivery because of the rate-capacity effect [17, 32]. To clearly demonstrate the rate-capacity effect, Fig. 10 shows our measurement results on discharging a 2,900mAh Lithium-ion cell with different currents. We can see that the delivered capacity when discharging the cell with a current of 1,000mA is about 187.7mAh less than that delivered with a discharge current of 200mA.

Without loss of generality, denote $H = \{h_1, h_2, \cdots, h_N\}$ as the estimated SoH levels for the N cells $\{b_1, b_2, \cdots, b_N\}$

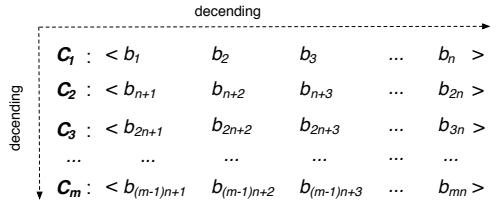

Figure 11: The obtained configuration with SHARE-Full.

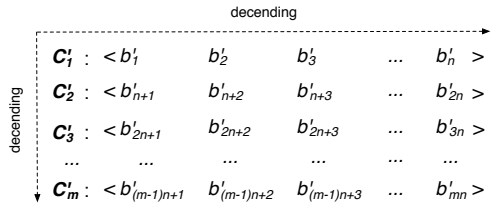

Figure 12: The optimal configuration.

in descending order, i.e., $\forall i < j \;\Rightarrow\; h_i \geq h_j$. Define an indicator variable $a_{i,j}$ as

$$a_{i,j} = \begin{cases} 1 & \text{if } b_i \in s_j \\ 0 & \text{otherwise.} \end{cases}$$

To capture the requirement on the disjoint strings, we further define the conflict relationship between two strings s_i and s_j as

$$conflict(s_i, s_j) = 1 \Longleftrightarrow \exists k \in \{1, 2, \cdots, N\},\ a_{k,i} \cdot a_{k,j} = 1,$$

Because the deliverable capacity of a series string is dominated by the cell with the lowest SoH levels, the deliverable capacity C_j for string s_j can be captured by

$$C_j = \min\{a_{i,j} \cdot h_i\}^+ \cdot c \quad (i = 1, 2, \cdots, N), \tag{1}$$

where $\min\{\cdot\}^+$ identifies the minimum non-zero value and c is the cell nominal capacity.

As a result, our objective to maximize the deliverable capacity can be formulated as

$$\max \sum_{j=1}^{m} C_j \tag{2}$$
$$s.t. \qquad \forall i, j,\ x_i \cdot x_j = 1 \implies conflict(s_i, s_j) = 0.$$

4.2 SHARE-Full

We propose SHARE-Full, a simple but efficient solution to solve the above problem and prove its optimality in delivering the maximum amount of capacity.

In SHARE-Full, we always select the n cells with the highest SoH levels to form the first cell string, and repeat the process in the remaining cells until all the m cell strings have been formed. In this way, one can see that $C_i = h_{(i\times n)}c$, and the totally deliverable capacity is $\sum_{i=1}^{m} h_{(i\times n)}c$. It is clear the time to sort the cells according to their SoH levels dominates the computation complexity of SHARE-Full, which is $\mathcal{O}(\log N)$. Next we will show that although simple, SHARE-Full achieves an optimal solution in terms of capacity delivery.

Theorem 1. For battery packs with full reconfigurability, SHARE-Full identifies the battery pack configuration with the maximum deliverable capacity.

Proof. The above theorem can be proven by contradictory. The cell configuration identified by the proposed solution can be arranged as in Fig. 11, where the top-n cells with the highest SoH levels (i.e., $\{b_1, b_2, \cdots, b_n\}$) form the first string with deliverable capacity C_1, and the second top-n cells $\{b_{n+1}, b_{n+2}, \cdots, b_{2n}\}$ form the second string with deliverable capacity C_2, etc. It is clear that

$$C_1 \geq C_2 \geq \cdots \geq C_m. \tag{3}$$

Assume there is another configuration that can deliver more capacity than that in Fig. 11, which is shown in Fig. 12. Without loss of generality, we assume

$$C'_1 \geq C'_2 \geq \cdots \geq C'_m. \tag{4}$$

If $\sum_{i=1}^{m} C'_i > \sum_{i=1}^{m} C_i$ holds, there must exist $j \in [1, m]$ such that $C'_j > C_j$. It is clear that $C_1 \geq C'_1$ because the first string identified by the proposed solution consists of the n cells with the highest SoH levels. If $C_2 < C'_2$, we know the cells forming the second string in Fig. 12 (i.e., $< b'_{n+1}, b'_{n+2}, \cdots, b'_{2n} >$) satisfy

1. $\forall b'_i \in \{b'_{n+1}, b'_{n+2}, \cdots, b'_{2n}\} \rightarrow b'_i \in \{b_1, b_2, \cdots, b_{2n}\}$;
2. $\exists b'_i \in \{b'_{n+1}, b'_{n+2}, \cdots, b'_{2n}\} \rightarrow b'_i \in \{b_1, b_2, \cdots, b_n\}$;
3. $b_{2n} \notin \{b'_{n+1}, b'_{n+2}, \cdots, b'_{2n}\}$.

However, when all the three conditions are satisfied, there is no solution to form the first string in Fig. 12 such that $C'_1 > C'_2$, which concludes that $C_2 \geq C'_2$. It can be proved in a similar manner that $\forall i, C_i \geq C'_i$, which contradicts the assumption that $\sum_{i=1}^{m} C'_i > \sum_{i=1}^{m} C_i$. As a result, the proposed solution identifies the configuration that delivers the maximum capacity, and thus its optimality is proved. □

5. BATTERY PACKS WITH PARTIAL RECONFIGURABILITY

In this section, we investigate the SoH-aware reconfiguration for battery packs with partial reconfigurability.

5.1 Problem Formulation

Unlike the case with fully reconfigurable battery packs where any n cells can be organized into a string, not any subset of n cells can be connected in series when the battery pack offers only partial reconfigurability. Thus the first step to identify the configuration with the maximum deliverable capacity is to identify all possible n-cell strings in the battery pack.

With the graph representation of the battery pack, we can transform the problem of identifying the n-cell strings in the battery pack to finding the simple paths consisting of n vertices in the corresponding graph G. Although it can be shown that finding all n-vertex paths in G is NP-hard by deducing it from the longest path problem [38], an $\mathcal{O}(\Delta^{n-1}N^{2.37})$ algorithm has been proposed in [18], where Δ is the out-degree of vertices in G. Furthermore, for reconfigurable battery packs, the number of cells that a specific cell can connect to is limited due to the constraint on system complexity [17]. This is reflected in G that Δ will not be large, which significantly reduces the computation complexity to identify these paths. Furthermore, with a given battery pack, all the n-cell strings can be identified offline and stored in the battery management system, and then

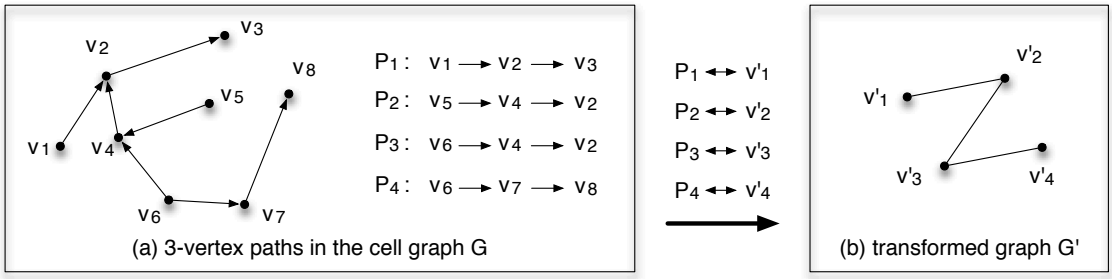

Figure 13: Graph transformation.

we only need to search through these pre-identified strings whenever the system reconfiguration is required.

Denote $\mathcal{P} = \{P_1, P_2, \cdots, P_M\}$ as the set of all n-vertex simple paths in the graph. Similar to the conflict relationship for two strings, the conflict relationship between two paths P_i and P_j is defined as

$$conflict(P_i, P_j) = 1 \Longleftrightarrow \exists k \in \{1, 2, \cdots, N\},\ a_{k,i} \cdot a_{k,j} = 1,$$

meaning that the two paths share certain common vertices (cells). Again, the conflicted paths should not be included in the final configuration, as explained in Section 4.

Denote x_i $(i = 1, 2, \cdots, M)$ as the indicator of whether P_i has been included in the final configuration

$$x_i = \begin{cases} 1 & \text{if } P_i \text{ is involved in the final configuration} \\ 0 & \text{otherwise.} \end{cases}$$

The deliverable capacity C_i of path P_i can be calculated in the same way as in Eq. (1). Therefore, our problem in maximizing the capacity delivery of the battery pack can be formulated as

$$\max \quad \mathcal{C} = \sum_{k=1}^{M} x_k \cdot C_k \tag{5}$$
$$s.t. \qquad \forall i, j, \quad x_i \cdot x_j = 1 \implies conflict(P_i, P_j) = 0.$$

5.2 Problem Transformation

To shed more light on the above problem formulation, we first perform the following problem transformation, which not only help us to show its NP-hardness, but also inspires us the design of a simple but efficient solution.

With the path set $\mathcal{P}$ and their conflicting relationship, we can construct another graph G' by

- mapping each $P_i \in \mathcal{P}$ to a vertex v'_i in G';
- an edge connecting any two vertices v'_i and v'_j in G' exist if and only if the two paths corresponding to the two vertices in the original graph G conflict with each other (i.e., $conflict(P_i, P_j) = 1$); and
- the weight on vertex v'_i in G' is the deliverable capacity C_i of the corresponding path in G.

Fig. 13 shows an example on the graph transformation. Consider the case where 3-cell strings are required to support the load. After constructing the graph representation of a 8-cell battery pack, four 3-vertex paths are found as shown in Fig. 13(a). With the graph transformation operations, the four paths (i.e., P_1, P_2, P_3, P_4) are mapped to four vertices in G' (i.e., v'_1, v'_2, v'_3, v'_4). Furthermore, because P_1 and P_2 share a common vertex v_2 in G, the corresponding vertices v'_1 (for P_1) and v'_2 (for P_2) are connected by an edge in G'. The existence of other edges in G' can be explained similarly.

With the new graph G', our problem in (6) can be transformed to identify a subset of vertices in G' with the maximum weight sum, and the requirement on the disjoint paths in G can be captured by the requirement on the independent vertex pair in G'. As a result, the problem can be transformed to *finding a subset of vertices in G' such that 1) no edges exist between any pair of vertices in the subset, and 2) the weight sum of vertices in the subset is the largest.* Clearly, this is the maximum-weight independent set problem [38], which is known to be NP-hard. With any given instance of the maximum-weight independent set problem, we can deduce it to a special case of our problem by reversing the graph transformation, which proves the NP-Hardness of our problem.

5.3 SHARE-Partial

Although the maximum-weight independent set problem is known to be NP-hard, it has been shown that the greedy solution for its non-weighted version achieves a solution with bounded optimality [16]. This inspires us the design of SHARE-Partial.

For each vertex v'_i in G', the gain to include it into the independent set is the amount of its deliverable capacity C_i. In SHARE-Partial, we greedily add the vertex v'_i with the largest C_i to the dominating set until no vertices can be included any more, i.e., a maximal independent set is formed. At last, the selected vertices are transformed back to the paths in the original graph, and the configuration of the battery pack is identified.

THEOREM 2. For battery packs with partial reconfigurability and in terms of maximizing their capacity delivery, SHARE-Partial achieves a performance ratio of

$$\frac{(\Delta' + 2) \cdot C_{\max}}{3 \cdot C_{\min}},$$

when compared with the optimal solution, where $C_{\max}$ and $C_{\min}$ are the largest and smallest deliverable capacity of all the n-cell strings, and Δ' is the maximal degree of vertices in the transformed graph G'.

It has been proved in [16] that a performance ratio of $\frac{\Delta+2}{3}$ can be achieved by the greedy solution for the maximum independent set problem (i.e., when vertices have uniform weight). The above theorem can be proved by incorporating the vertices weight into the proof therein, which is not included here due to the space limit.

Table 2: SoH levels of adopted cells.

Cell	#1	#2	#3	#4	#5
Cap. (mAh)	1781.7	2188.0	2224.5	1841.4	1721.2
SoH (%)	77.5	95.1	96.7	80.1	74.8
Cell	#6	#7	#8	#9	#10
Cap. (mAh)	2224.5	1911.2	2224.2	1802.2	2139.5
SoH (%)	96.7	83.1	96.7	78.4	93.0
Cell	#11	#12	#13	#14	#15
Cap. (mAh)	2291.4	1791.6	1805.0	2205.7	2142.2
SoH (%)	99.6	77.9	78.5	95.9	93.1

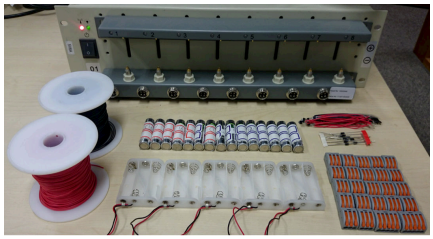

Figure 14: Laboratory settings for the experiments.

6. EXPERIMENT EVALUATIONS

In this section, we experimentally evaluate the performance of SHARE-Full and SHARE-Partial, respectively.

6.1 Experiment Settings

• **Cells and SoH Levels:** We form a 15-cell battery pack with 2,300mAh AA rechargeable cells. We discharge these cells with a 1C current after fully charge and record their respectively delivered capacity, based on which their SoH levels are estimated as shown in Table 2. Fig. 14 shows the laboratory settings for the experiments.

• **Loads:** In the experiment, we consider the case where 3-cell strings are required to support the load, which demands a total discharge current of 2,300mA. Again, the NEWARE battery testing system is adopted to explicitly control the discharge current.

• **Battery Packs:** We emulate three battery packs with different reconfigurability. First, a *non-reconfigurable battery pack* where five 3-cell strings are formed by cells $\{\overline{1,2,3}\}$, $\{\overline{4,5,6}\}$, $\{\overline{7,8,9}\}$, $\{\overline{10,11,12}\}$, and $\{\overline{13,14,15}\}$, respectively. In other words, the cells are connected sequentially according to their indexes without the consideration of their SoH levels. Second, a *partially reconfigurable battery pack* which is constructed on top of the sequential configuration by allowing each cell to connect to another randomly selected cell. Specifically, the connectivity matrix of the partially reconfigurable battery pack is shown in Fig. 15. Third, a fully reconfigurable battery pack where any subset of cells can be connected in series.

$$\begin{bmatrix}
- & 1 & 0 & 0 & 0 & 0 & 0 & 0 & 1 & 0 & 0 & 0 & 0 & 0 & 0 \\
0 & - & 1 & 0 & 0 & 0 & 0 & 0 & 0 & 0 & 1 & 0 & 0 & 0 & 0 \\
0 & 0 & - & 1 & 0 & 0 & 0 & 0 & 0 & 0 & 1 & 0 & 0 & 0 & 0 \\
0 & 0 & 0 & - & 1 & 1 & 0 & 0 & 0 & 0 & 0 & 0 & 0 & 0 & 0 \\
0 & 0 & 0 & 0 & - & 1 & 0 & 0 & 0 & 0 & 1 & 0 & 0 & 0 & 0 \\
0 & 0 & 1 & 0 & 0 & - & 1 & 0 & 0 & 0 & 0 & 0 & 0 & 0 & 0 \\
0 & 1 & 0 & 0 & 0 & 0 & - & 1 & 0 & 0 & 0 & 0 & 0 & 0 & 0 \\
0 & 1 & 0 & 0 & 0 & 0 & 0 & - & 1 & 0 & 0 & 0 & 0 & 0 & 0 \\
0 & 0 & 0 & 0 & 0 & 0 & 0 & 0 & - & 1 & 1 & 0 & 0 & 0 & 0 \\
0 & 0 & 0 & 0 & 0 & 0 & 0 & 0 & 1 & - & 1 & 0 & 0 & 0 & 0 \\
1 & 0 & 0 & 0 & 0 & 0 & 0 & 0 & 0 & 0 & - & 1 & 0 & 0 & 0 \\
0 & 0 & 0 & 0 & 0 & 0 & 0 & 0 & 0 & 0 & 0 & - & 1 & 1 & 0 \\
0 & 0 & 0 & 0 & 0 & 0 & 0 & 0 & 0 & 1 & 0 & 0 & - & 1 & 0 \\
0 & 0 & 0 & 0 & 0 & 1 & 0 & 0 & 0 & 0 & 0 & 0 & 0 & - & 1 \\
0 & 0 & 0 & 0 & 0 & 0 & 0 & 0 & 1 & 0 & 0 & 0 & 0 & 0 & -
\end{bmatrix}$$

Figure 15: Adjacent matrix of the partially reconfigurable battery pack.

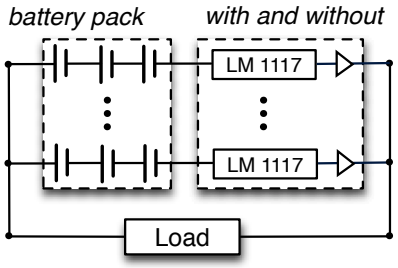

Figure 16: Experiment methodology.

Table 3: Delivered capacities (mAh).

Configuration	w/o Regulator	w/ Regulator
SHARE-Full	10,743.4	6,214.2
SHARE-Partial	10,385.6	5,959.8
SoH-oblivious	9,758.7	5,647.6

We apply SHARE-Full and SHARE-Partial onto the fully and partially reconfigurable battery packs, respectively. The obtained SoH-aware configurations are:

$$\text{Fully}: \overline{\{11,6,8\}}||\overline{\{3,14,2\}}||\overline{\{15,10,7\}}||\overline{\{4,13,9\}}||\overline{\{12,1,5\}},$$
$$\text{Partially}: \overline{\{7,8,15\}}||\overline{\{9,10,11\}}||\overline{\{2,13,14\}}||\overline{\{3,4,5\}}||\overline{\{1,6,12\}}.$$

Then we connect the cells according to the obtained configurations to support the loads, and the discharge process terminates when the output voltage of the battery packs reduces to 1.5 V.

• **Methodologies:** Our experiments consist of two parts as illustrated in Fig. 16. In the first set of experiments, the fully charged battery packs are directly connected to the load, which assists to reveal the fundamental impact of the SoH-aware configuration on the deliverable capacities of the battery packs. In the second set of experiments, a LM 1117 voltage regulator and a protection diode is inserted between each of the 3-cell string and the load, as in most practical applications with parallel connected strings. This experiment setting helps to reveal the practical effect of the SoH-aware configuration in enhancing the capacity delivery.

6.2 Experiment Results

The experiment results with different settings and different emulated battery packs are summarized in Table 3. Taking the traditional SoH-oblivious configuration as the baseline, when directly connecting the battery packs with the loads, the improvement ratios in terms of the delivered capacity are 10.1% and 6.5% with the fully and partially reconfigurable battery packs. These improvement ratios are 10% and 5.5%, respectively, when the voltage regulators and diodes are adopted in the experiment settings.

Further comparing the two experiment settings (i.e., w/ and w/o regulators), we can see that the amount of delivered capacities are largely reduced when the regulators and the protection diodes are adopted. This is because the involvement of these complimentary components introduces non-negligible energy loss, and thus reduces the capacity that can be drawn to actually support the loads.

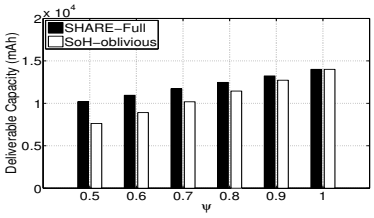

Figure 17: Deliverable capacity with imbalance degree in a fully reconfigurable battery pack.

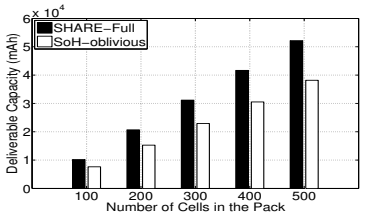

Figure 18: Deliverable capacity with the number of cells of a fully reconfigurable battery pack.

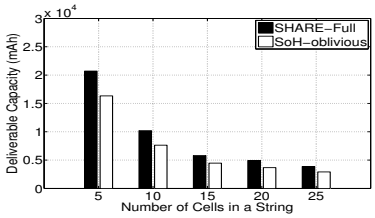

Figure 19: Deliverable capacity with string size in a fully reconfigurable battery pack.

7. SIMULATION EVALUATIONS

In this section, we evaluate SHARE-Full and SHARE-Partial through extensive simulations.

7.1 Fully Reconfigurable Battery Pack

In the evaluation of SHARE-Full, we simulate a battery pack consisting of 100–500 cells, each with a nominal capacity of $1,400$mAh. The size of the cell string n (i.e., the number of cells in a string) to support the load varies from 5 to 25.

A control parameter $\psi \in [0, 1]$ is introduced to capture the imbalance degree of cells in the battery pack. Specifically, in our simulator, the SoH levels of cells are randomly generated in the range of

$$[\psi, 1] \times 100\%.$$

For example, the SoH levels of the cells adopted in our experiment (Table 2) can be captured by a case of $\psi = 0.7$. Clearly, a smaller ψ indicates more severe cell imbalance.

Similar to the non-reconfigurable battery pack emulated in Section 6.1, we also implement a SoH-oblivious configuration where the cell strings are formed sequentially according to the cell index and is non-reconfigurable, i.e., the 1st to the nth cells form the 1st cell string, the $(n+1)$th to the $(2n)$th cells form the 2nd cell string, etc. The results and observations reported below are averaged over a total number of 100 simulation runs.

• **Impact of Cell Imbalance Degree:** SHARE-Full is proposed to address the cell imbalance in the battery pack, and thus we first evaluate its performance with varying imbalance degree of cells. The deliverable capacity with SHARE-Full and the SoH-oblivious configuration for a 100-cell battery pack are shown in Fig. 17, where ψ varies from 0.5 to 1.

Significantly larger amount of capacity can be delivered with SHARE-Full when compared with the SoH-oblivious configuration, especially with severe cell imbalance (i.e., with a smaller ψ). For example, with a ψ of 0.8, SHARE-Full delivers about $12,463 - 11,444 = 1,019$mAh more capacity than the SoH-oblivious configuration, indicating an increase ratio of about $\frac{1,019}{11,444} = 8.9\%$, and this increase become even more significant with a ψ of 0.5, i.e., $10,188 - 7,625 = 2,563$mAh and about $\frac{2,563}{7,625} = 33.6\%$. These observations validate the effectiveness of SHARE-Full in mitigating the cell imbalance in battery packs.

• **Impact of Battery Pack Size:** Next we investigate the impact of battery pack size on the performance of SHARE-Full. With a string size of 10 and a cell imbalance degree $\psi = 0.5$, the deliverable capacity with varying battery pack size from 100–500 are shown in Fig. 18.

As can be clearly observed, more capacity can be delivered with SHARE-Full, and its advantage becomes more obvious as the size of the battery pack increases. Specifically, when compared with the SoH-oblivious configuration, an increase ratio in the deliverable capacity of about $\frac{10,186-7,631}{7,631} = 33.48\%$ can be obtained with a 100-cell battery pack, which further increases to about $\frac{52,155-38,171}{38,171} = 36.64\%$ when the size of the battery pack increases to 500. These observations demonstrate the necessity of the SoH-aware configuration especially for large-scale battery systems.

• **Impact of String Size:** With a 100-cell battery pack, the deliverable capacity with string size varies from 5 to 25 are shown in Fig. 19. We can see the advantage of SHARE-Full is more obvious with a smaller string size. This is intuitive because a smaller string size leads to a larger number of parallel connected strings, which enlarges the effectiveness of SHARE-Full in forming stronger strings. Even though the increased deliverable capacity in the case of a 25-cell string is relatively small (i.e., $3,868 - 2,909 = 959$mAh), the increase ratio when compared with the SoH-oblivious configuration is still significant (i.e., 33.0%).

7.2 Partially Reconfigurable Battery Pack

Next we evaluate the performance of SHARE-Partial for partially reconfigurable battery packs.

Most simulation settings for the partially reconfigurable battery packs are the same as in the case of fully reconfigurable battery packs, and the main difference is on how to implement the partial reconfigurability.

Our observation when implementing the partially reconfigurable battery packs is that the most straightforward configuration among cells, i.e., connecting cells sequentially according to their respective index as in the non-reconfigurable battery pack in Section 7.1, is supported by most *off-the-shelf* battery packs. As a result, we implement the partial reconfigurability on top of this sequential configuration in our simulator by additionally adding a number of α relays to each cell, which allows them to connect to α randomly selected other cells (i.e., $\alpha = 1$ for the partially reconfigurable battery pack as in Section 6.1). Specifically, in terms of the connectivity matrix of the corresponding graph representation, the sequential configuration in a N-cell pack can be captured by

$$\mathcal{Y}_{N\times N} = \{y_{i,j}\} = \begin{cases} 1 & \text{if } j = i+1 \\ 0 & \text{otherwise,} \end{cases}$$

and we generate the partially reconfigurable battery pack by randomly selecting α non-diagonal 0s in each row of $\mathcal{Y}_{N\times N}$ and updating them to 1. In this way, one can see that the number of additionally involved relays α trades off between the system reconfigurability and complexity.

• **Impact of Cell Imbalance Degree:** Again, we first evaluate the impact of cell imbalance degree on the performance of SHARE-Partial. With a battery pack consist-

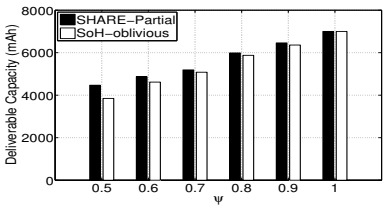

Figure 20: Deliverable capacity with imbalance degree in a partially reconfigurable battery pack.

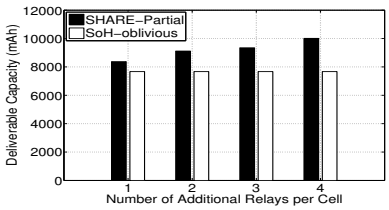

Figure 21: Deliverable capacity with the number of relays in a partially reconfigurable battery pack.

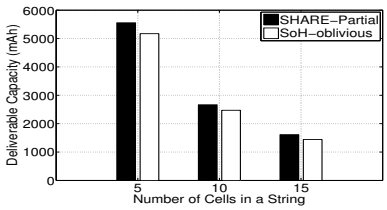

Figure 22: Deliverable capacity with string size in a partially reconfigurable battery pack.

ing of 50 cells each with a nominal capacity of $1,400$mAh, the deliverable capacity with SHARE-Partial and the SoH-oblivious configuration are shown in Fig. 20. The cell imbalance degree ψ is 0.5, the string size is 10, and $\alpha = 1$.

One can see that even with only 1 additionally involved relays for each cell, a significant improvement in the deliverable capacity can be observed with SHARE-Partial, which becomes more obvious with a more severe cell imbalance issue. For example, about $4,468 - 3,848 = 620$mAh more capacity can be delivered with $\psi = 0.5$, corresponding to an increase ratio of about $\frac{620}{3,848} = 16.1\%$ when compared with the SoH-oblivious configuration. However, this increase is not as large as for fully reconfigurable battery packs because of a much lower system reconfigurability.

• **Impact of Reconfigurability:** Next we investigate the impact of the reconfigurability on SHARE-Partial. Fig. 21 shows the deliverable capacity with α varies from 1 to 4, where the sizes of the battery pack and the cell strings are 50 and 5, respectively. The cell imbalance degree ψ is 0.5. The first observation is that the deliverable capacity with SHARE-Partial increases as higher reconfigurability is offered by the battery pack. For example, the deliverable capacity increases from $8,373$mAh to $10,013$mAh when α increases from 1 to 4. Furthermore, when compared with the SoH-oblivious configuration, the advantage of SHARE-Partial becomes more obvious as α increases. However, because a larger α leads to higher system complexity, offering a proper level of reconfigurability with the joint consideration of energy efficiency and system complexity is of significant practical value, which is the direction of our further investigation.

• **Impact of String Size:** The delivered capacity with string size varying from 5 to 15 are shown in Fig. 22, with a simulated 30-cell battery pack where $\psi = 0.5$ and $\alpha = 1$. We can see about 383mAh, 194mAh, and 172mAh more capacity can be delivered with SHARE-Partial when the string size is 5, 10, and 15, respectively. Although the improvement is not as obvious as for the fully reconfigurable battery packs due to the much lower reconfigurability, the improvement ratio when compared with the SoH-oblivious configuration is still observable, i.e., 7.4%–11.9%.

8. CHANGES OF CELL VOLTAGES

As shown in Fig. 4, in this paper, we consider the system model where strings consisting of a fixed number of cells (determined based on the nominal voltage of cells and the load required voltage) are required to support the load, with the assistance of a voltage regulator. This is the common system model for commercial battery packs such as the AMP20 Energy Modules by A123 Systems [1]. However, the cell voltage will deviate from its nominal level during discharging, which increases the gap between the string supplied and the load required voltages and thus degrades the voltage regulating efficiency [3, 4].

For battery packs with full reconfigurability, the changes of cell voltages can be easily handled with SHARE-Full by adaptively adjusting the number of cells in a string so as to match the load required voltage. For partially reconfigurable battery packs, dynamically constructing cell strings to achieve an output voltage close to the load required level is a straightforward approach to address this issue, which have been investigated in previous work [17]. The design therein can be incorporated into SHARE-Partial by changing the definition of the path set $\mathcal{P}$ in Section 5.1–instead of identifying all n-vertex paths in the graph, we can assign each vertex another weight (besides the weight capturing the cell SoH) according to their real-time voltage levels, and form $\mathcal{P}$ only with the paths whose weight sum is close to the load requirements. Then the SoH-aware reconfiguration can be performed in the same way based on the newly identified path set $\mathcal{P}$. This approach also helps to mitigate the issue of various voltage levels among cells, which is likely to occur because of the cell imbalance in the pack.

9. RELATED WORK

With the wide adoption of battery systems such as electric vehicles and aircraft [2, 6, 30, 39], significant research effort has been devoted to improving the system performance through effective system monitoring [25], advanced design of battery management systems [13, 21, 31, 35, 36], optimal battery discharge scheduling [11, 12, 14, 23, 33, 42], etc.

Recently, the concept and implementation of reconfigurable battery packs have be attracting increasing attentions from both academia and industry [1, 7, 22, 27], because of their advantages in higher efficiency [15, 17, 18, 29], stronger robustness [20], and easier management [24].

A reconfiguration architecture aiming at cycle efficiency and capacity utilization enhancement is proposed in [29]. Kim *et al.* [24] proposed a scalable architecture for the management of large-scale battery packs. The efficient monitoring of the battery system has been investigated in [25]. In [20], a *power tree* representation of the battery pack is proposed to assist the effective system reconfiguration when the battery failures happen. A reconfigurable series-connected battery string is proposed in [26] to adjust the supplied voltage to the load required level. The additional consideration on minimizing the discharge current of individual battery cells is incorporated into the reconfiguration design in [17]. Utilizing the battery pack reconfigurability to assist in charging the battery cells to their fully capacity has been investigated in [18], where a reconfiguration-assisted charging algorithm is proposed and empirically evaluated.

Different from these existing studies, in this paper, we explore the feasibility of utilizing the battery pack reconfig-

urability together with the cells' SoH levels, to mitigate the notorious cell unbalance issue, which is known to dramatically degrade the energy efficiency and even risk the safety of the entire system.

10. CONCLUSION

In this paper, we mitigate cell imbalance via SoH-aware reconfiguration in battery packs, which jointly explores the system reconfigurability and the state-of-health of cells to enhance the capacity delivery of battery packs, which in turn extends the system operation time. We have proposed two SoH-aware configuration algorithms, SHARE-Full and SHARE-Partial, focusing on fully and partially reconfigurable battery packs, respectively. We have evaluated the performance of SHARE-Full and SHARE-Partial using both experiments and simulation. The results demonstrate that about 10–30% more capacity can be delivered than SoH-oblivious configurations.

Acknowledgment: The work reported in this paper was supported in part by NSF under Grants CNS-1329702, CNS-1446117, and CNS-1503590.

11. REFERENCES

[1] AHR32113 Power Modules. `http://www.a123systems.com/products-modules-power.htm`.

[2] Air Craft Battery Pack. `http://www.jc-aviation.com/aircraft_battery_power_packs.html`.

[3] Energy Loss on Regulators. `http://www.dimensionengineering.com/info/switching-regulators`.

[4] Linear Voltage Regulator. `http://www.eefocus.com/data/07-07/26\_1183518457/File/1183615093.pdf`.

[5] Neware Battery Testing System. `http://www.youtube.com/watchv=NAVrm3wjzq8`.

[6] Pursuing a battery so electric vehicles can go the extra miles. `http://www.nytimes.com/2009/09/15/science/15batt.html`.

[7] Reconfigurable Battery Packs. `http://arpa-e.energy.gov/q=arpa-e-projects/reconfigurable-battery-packs`.

[8] Why Your Battery Life is Terrible, in One Handy Chart. `http://www.technologyreview.com/view/424996/why-your-battery-life-is-terrible-in-one-handy-chart/`.

[9] Hybrid Cars. *First numbers on hybrid battery failure*, 2008.

[10] D. Andrea. Battery management systems for large Lithium-ion battery packs. *Artech House*, 2010.

[11] L. Benini, G. Castelli, A. Macii, B. Macii, and R. Scarai. Battery-driven dynamic power management of portable systems. In *ISSS'00*, 2000.

[12] G. Castelli, A. Macii, E. Macii, and M. Poncino. Current-controlled policies for battery-driven dynamic power management. In *ICECS'01*, 2001.

[13] C. F. Chiasserini and R. Rao. Energy efficient battery management. *IEEE Journal on Selected Areas in Communications*, 19(7):1235–1245, 2001.

[14] C. F. Chiasserini and R. Rao. Improving battery performance by using traffic shaping techniques. *IEEE Journal on Selected Areas in Communications*, 19:1385–1394, 2001.

[15] S. Ci, J. Zhang, H. Sharif, and M. Alahmad. Dynamic reconfigurable multi-cell battery: A novel approach to improve battery performance. In *APEC'12*, 2012.

[16] M. M. Halldorsson and J. Radhakrishnan. Greed is good: Approximating independent sets in sparse and bounded-degree graphs. *Algorithmica*, 18:145–163, 1997.

[17] L. He, L. Gu, L. Kong, Y. Gu, C. Liu, and T. He. Exploring adaptive reconfiguration to optimize energy efficiency in large-scale battery systems. In *RTSS'13*, 2013.

[18] L. He, L. Kong, S. Lin, S. Ying, Y. Gu, T. He, and C. Liu. Reconfiguration-assisted charging in large-scale Lithium-ion battery systems. In *ICCPS'14*, 2014.

[19] L. He, S. Ying, and Y. Gu. Demo: Reconfiguration-based energy optimization in battery systems: a testbed prototype. In *RTSS@Work'13*, 2013.

[20] F. Jin and K. G. Shin. Pack sizing and reconfiguration for management of large-scale batteries. In *ICCPS'12*, 2012.

[21] E. Kim, J. Lee, and K. G. Shin. Real-time battery thermal management for electric vehicles. In *ICCPS'14*, 2014.

[22] H. Kim and K. G. Shin. On dynamic reconfiguration of a large-scale battery system. In *RTAS'09*, 2009.

[23] H. Kim and K. G. Shin. Scheduling of battery charge, discharge, and rest. In *RTSS'09*, 2009.

[24] H. Kim and K. G. Shin. Dependable, efficient, scalable architecture for management of large-scale batteries. In *ICCPS'10*, 2010.

[25] H. Kim and K. G. Shin. Efficient sensing matters a lot for large-scale batteries. In *ICCPS'11*, 2011.

[26] T. Kim, W. Qiao, and L. Qu. Series-connected self-reconfigurable multicell battery. In *APEC'11*, 2011.

[27] T. Kim, W. Qiao, and L. Qu. Power electronics-enabled self-X multicell batteries: A design toward smart batteries. *IEEE Transactions on Power Electronics*, 27(11):4723–4733, 2012.

[28] T. Kim, W. Qiao, and L. Qu. A series-connected self-reconfigurable multicell battery capable of safe and effective charging/discharging and balancing operations. In *APEC'12*, 2012.

[29] Y. Kim, S. Park, Y. Wang, Q. Xie, N. Chang, M. Poncino, and M. Pedram. Balanced reconfiguration of storage banks in a hybrid electrical energy storage system. In *ICCAD'11*, 2011.

[30] Z. Li, M. Li, J. Wang, and Z. Cao. Ubiquitous data collection for mobile users in wireless sensor networks. In *INFOCOM'11*, 2011.

[31] D. Lim and A. Anbuky. A distributed industrial battery management network. *IEEE Transactions on Industrial Electronics*, 51(6):1181–1193, 2004.

[32] D. Linden and T. B. Reddy. Handbook of Batteries (3rd ed.). *McGraw-Hill*, 2001.

[33] J. Luo and N. Jha. Battery-aware static scheduling for distributed real-time embedded systems. In *DAC'01*, 2001.

[34] S. J. Moura, J. L. Stein, and H. K. Fathy. Battery-health conscious power management in plug-in hybrid electric vehicles via electrochemical modeling and stochastic control. *IEEE Transactions on Control Systems Technology*, 21(3):679–694, 2013.

[35] S. Mukhopadhyay and F. Zhang. A high-gain adaptive observer for detecting Li-ion battery terminal voltage collapse. *Automatica*, 50(3):896 – 902, 2014.

[36] D. Rakhmatov and S. Vrudhula. Energy management for battery-powered embedded systems. *ACM Transactions on Embedded Computing Systems*, 2:277–324, 2003.

[37] D. Raychev, Y. Li, and W. Shi. The seventh cell of a six-cell battery. In *WEED'11*, 2011.

[38] D. Reinhard. Graph Theory (3rd ed.). *Springer*, 2005.

[39] D.-H. Shin, S. He, and J. Zhang. Robust, secure, and cost-effective design for cyber-physical systems. *IEEE Intelligent Systems*, 29(1):66–69, 2014.

[40] J. L. Vian, A. R. Mansouri, R. Elangovan, M. M. Borumand, and K. Abdel-Motagaly. Health Management of Rechargeable Batteries. *US patent, 2010/0121587*, 2010.

[41] S. Zeljkovic, T. Reiter, and D. Gerling. Efficiency optimized single-stage reconfigurable DC/DC converter for hybrid and electric vehicles. *Emerging and Selected Topics in Power Electronics, IEEE Journal of*, 2(3):496–506, Sept 2014.

[42] F. Zhang and Z. Shi. Optimal and adaptive battery discharge strategies for cyber-physical systems. In *CDC'09*, 2009.